BAMS Article

A New Predictive Framework for Amazon Forest Fire Smoke Dispersion over South America

Angel Liduvino Vara-Vela, Dirceu Luís Herdies, Débora Souza Alvim, Éder Paulo Vendrasco, Silvio Nilo Figueroa, Jayant Pendharkar, and Julio Pablo Reyes Fernandez

ABSTRACT: Aerosol particles from forest fire events in the Amazon can be effectively transported to urban areas in southeastern South America, thus affecting the air quality over those regions. A combination of observational data and a comprehensive air quality modeling system capable of anticipating acute air pollution episodes is therefore required. A new predictive framework for Amazon forest fire smoke dispersion over South America has been developed based on the Weather Research and Forecasting with Chemistry community (WRF-Chem) model. Two experiments of 48-h simulations over South America were performed by using this system at 20-km horizontal resolution, on a daily basis, during August and September of 2018 and 2019. The experiment in 2019 included the very strong 3-week forest fire event, when the São Paulo metropolitan area, located in southeastern South America, was plunged into darkness on August 19. The model results were satisfactorily compared against satellite-based data products and in situ measurements collected from air quality monitoring sites. The system is executed daily immediately after the CPTEC Satellite Division releases the latest active fire locations data and provides 48-h forecasts of regional distributions of chemical species such as CO, $PM_{2.5}$, and O_3. The new modeling system will be used as a benchmark within the framework of the Chemistry of the Atmosphere–Field Experiment in Brazil (CAFE-Brazil) project, which will take place in 2022 over the Amazon.

KEYWORDS: Model evaluation/performance; Regional models; Aerosols/particulates; Air pollution; Air quality; Atmospheric composition

https://doi.org/10.1175/BAMS-D-21-0018.1
Corresponding author: Dirceu L. Herdies, dirceu.herdies@inpe.br, dherdies@gmail.com
Supplemental material: https://doi.org/10.1175/BAMS-D-21-0018.2

In final form 30 April 2021

AFFILIATIONS: Vara-Vela, Herdies, Alvim, Vendrasco, Figueroa, Pendharkar, and Fernandez—Center for Weather Forecasting and Climate Studies, National Institute for Space Research, Cachoeira Paulista, São Paulo, Brazil

Biomass-burning episodes are quite common in the central Amazon and represent a dominant source of aerosols during the dry season, between August and October (Artaxo et al. 2002; Hoelzemann et al. 2009; Alvim et al. 2017). These episodes have local and regional impacts as well as global impacts once their emissions disrupt the carbon cycle, in addition to causing changes in the world's rainfall regime (Ichoku et al. 2012; Belcher 2013). The injection of large amounts of trace gases and aerosols into the atmosphere from the fire events in the Amazon can then be effectively transported to urban areas in southeastern South America (Freitas et al. 2005; Martins et al. 2018), thus affecting the air quality over those regions. Air pollution from biomass burning in the Amazon is estimated to cause an average of approximately 3,000 premature deaths per year across South America (Reddington et al. 2015), in addition to the melting of tropical Andean glaciers (de Magalhães et al. 2019), reductions in agricultural productivity as a result of increases in surface ozone concentrations (Pacifico et al. 2015; Gonzalez-Alonso et al. 2019), and low-visibility conditions at airports and highways.

One of the main ways to study and evaluate the air pollution induced by biomass burning and other emission sources is through future projections of the atmospheric state, including their disturbances. These projections are obtained with mathematical models on supercomputers. Hence, to obtain results that are physically consistent with observations, atmospheric models must correctly incorporate the emissions sources and accurately simulate the transport of these emissions and their interactions with the environment. The state-of-the-art Advanced Research version of the Weather Research and Forecasting (WRF-ARW; Skamarock et al. 2008) Model configured with three one-way nested grids with 9-, 3- and 1-km horizontal resolutions (South America: 9 km; southeastern Brazil: 3 km; and Rio de Janeiro–Guanabara Bay: 1 km) was implemented operationally at the Center for Weather Forecasting and Climate Studies (CPTEC) during the 2016 Olympic Games in Rio de Janeiro to support the sailing competitions in Guanabara Bay. After successfully forecasting surface winds during the 2016 Rio Olympics, this system continued to be operational until 2017. Subsequently, the WRF-ARW-5km system was adapted for South American land, topography, and vegetation conditions and tested for 17 different physics schemes to choose the best configuration for operational use (Table 1). Since 2018, the WRF-ARW-5km has been the new regional numerical weather prediction (NWP) model at CPTEC for 72-h forecasts over South America and the tropical Atlantic Ocean.

Recently, a new predictive framework for the dispersion of smoke from Amazon forest fires over South America has been developed based on coupling the WRF-ARW with a chemistry model (WRF-Chem; Grell et al. 2005). Due to its robustness and versatility, a vast number of weather services across the world have used the WRF-Chem model for operational forecasts and research (e.g., Solazzo et al. 2017; Eric et al. 2018; Petersen et al. 2019). Weather and atmospheric composition forecasts derived from the proposed modeling framework represent relevant information for atmospheric scientists and policy-makers looking at regional air quality management, particularly during the outbreak of large-scale forest fires. In addition, atmospheric simulations based on this new system will be used to guide High Altitude and Long range research aircraft (HALO) missions, which will take place over the Amazon in 2022 (https://halo-research.de/sience/previous-missions/). As part of the Chemistry of the Atmosphere–Field Experiment in Brazil (CAFE-Brazil) project, HALO experiments will facilitate the deployment of comprehensive sets of airborne instrumentation in order to better characterize transport, radiation, and chemical processes from regional to continental scales.

Table 1. Model setup. The physics schemes are based on the CPTEC WRF-ARW-5km regional NWP system (https://previsaonumerica.cptec.inpe.br/wrf).

Attribute	Scheme	Model option/coverage
Physics	Longwave and shortwave radiation	RRTMG
	Surface layer	Revised Monin–Obukhov
	Land surface	Unified Noah
	Boundary layer	YSU
	Cumulus	New Tiedtke
	Microphysics	Ferrier[a]
Chemistry	Gas-phase chemistry	MOZART
	Aerosol model	GOCART
	Dry deposition	Wesely
	Advection	Positive-definite and monotonic
Emissions	Anthropogenic	HTAPv2.2
	Biomass burning	3BEM[b]
Simulation design	Model version	3.9.1.1
	Spatial domain	South America
	Horizontal and vertical resolution	20 km—30 levels
	Initial and boundary conditions	GFS[c] (0.25°) and WACCM (0.9° × 1.25°)
	Simulation period	August and September of 2018 and 2019
	Variables for model evaluation	AOD_{550nm},[d] CO, O_3, $PM_{2.5}$, and precipitation

[a] No wet deposition is handled with Ferrier microphysics.

[b] Includes a sub-gridscale plume rise algorithm.

[c] NOAA's next-generation Global Forecast System model, known as GFS-FV3 (FV3 stands for finite volume cubed-sphere dynamical core) and put into operation on 12 Jun 2019, is used for the study period in 2019.

[d] For comparison with MODIS, the predicted AOD_{550nm} is derived from the CPTEC WRF-Chem AOD at 300-, 400-, and 999-nm wavelengths using the Angstrom power law [Eqs. (ES1) and (ES2) in the supplement].

The main goals of the present study are (i) to describe the new modeling framework for Amazon forest fire smoke dispersion over South America implemented at CPTEC, aiming to provide air pollution forecasts of CO, $PM_{2.5}$, O_3, and aerosol optical depth (AOD) based on near-real-time biomass-burning emissions; (ii) to evaluate the model performance for the August–September period in 2018 and 2019 in comparison to satellite observations; and (iii) to investigate how extreme Amazonian wildfire events can affect the atmospheric composition over the São Paulo metropolitan area (SPMA). The Amazon fire season and the new system, hereafter referred to as CPTEC WRF-Chem, are described in the second and third sections, respectively. The model evaluation and the unusual event over the SPMA are presented in the fourth section, and the conclusions are presented in the fifth section.

Amazon fire season

The Amazon, one of the world's most important tropical regions, is in continuous distress due to increased human occupation, expansion of agricultural activities, and climate change (Morgan et al. 2019). While deforestation in the Amazon normally peaks between May and July, the rise in the occurrence of fires coincides with the months of lowest rainfall, between August and September (Aragão et al. 2008). Although it spreads across several South American countries, more than half of the Amazon is in Brazil, where 80% of the area is covered by forest, whereas savanna and grassland biomes comprise 16% (Morgan et al. 2019; Devecchi et al. 2020). Deforestation rates, active fire counts, and burned area over the Brazilian Amazon significantly slowed after 2004, with peaks in active fire counts in 2005, 2007, and 2010 being more associated with extreme drought events than deforestation

(Tyukavina et al. 2017). However, significant increases in burned area in recent years point to a shift in fire dynamics and agricultural practices across the region (Barlow et al. 2019; Cardil et al. 2020). According to Lizundia-Loiola et al. (2020), the total burned area over the Brazilian Amazon in 2019 was 2.2 times larger than the burned area estimated for 2018, although very similar to the average of the time series 2001–18, with only 1.7% increase. They also found that among the countries more intensively affected by fires in the continent (Argentina, Brazil, Bolivia, Colombia, Paraguay, and Venezuela), the total burned area in 2019 was 1.71 times larger than in 2018, but only 1.05 larger than the average of the time series 2001–18. Figure ES1 in the online supplement (https://doi.org/10.1175/BAMS-D-21-0018.2) shows the spatial distributions of the Brazilian Biomass Burning Emission Model (3BEM) total burned area over South America during August and September of 2018 and 2019. The 3BEM model is the biomass-burning emissions component of the modeling system, and more details about it are given in the "The CPTEC WRF-Chem modeling system" section.

In general, the fire intensity over the Amazon emanates from forest, savanna, and grassland biomes (Kganyago et al. 2020), with forest having higher emission factors for particulate matter and nonmethane volatile organic compounds (NMVOCs) compared to savanna and grassland, both having the same emission factors (Andreae and Merlet 2001). The increase in the occurrence of fires in 2019 in the world's largest biomes has captured the attention of the international community. Active fire data from the National Aeronautics and Space Administration (NASA) Moderate Resolution Imaging Spectroradiometer (MODIS) sensors show that three biomes were particularly affected by fires in August 2019: the tundra, including low vegetation in several regions of Russia; the savanna, which covers much of Angola, the Democratic Republic of Congo, and Zambia; and the Amazon, which was hit mainly by fires concentrated in Brazil, Peru, and Bolivia, as reported by Voiland (2019). In addition, a rare and extreme smoke-related event occurred in the afternoon of Monday, 19 August 2019, in the most populous city in the Western Hemisphere, the SPMA, located in southeastern Brazil, with an average elevation of approximately 760 m above sea level. The sky over the SPMA suddenly blackened, with the day turning into night, as reported by Bloomberg News (see Fig. ES2 in the supplement).

The CPTEC WRF-Chem modeling system

The core component of the CPTEC WRF-Chem modeling system is the WRF-Chem model, which is a fully coupled meteorology–chemistry transport model used to simultaneously simulate meteorology, chemistry, and aerosol feedback effects at a regional scale and includes many aerosol and gas-phase chemistry schemes (https://ruc.noaa.gov/wrf/wrf-chem/).

For the modeling framework proposed here, the Model for Ozone And Related chemical Tracers (MOZART; Emmons et al. 2010) gas-phase and Goddard Chemistry Aerosol Radiation and Transport (GOCART; Chin et al. 2000) aerosol mechanisms are used. Tropospheric chemistry in MOZART is represented by 81 chemical species, which participate in 38 photolysis and 159 gas-phase reactions (Emmons et al. 2010). MOZART NMVOCs with an explicit representation include ethane, propane, ethene, propene, methanol, isoprene, and α-pinene. Other NMVOCs are lumped based on the reactive functional groups (Mar et al. 2016). The GOCART model simulates major tropospheric aerosol types, including sulfate, dust, organic carbon, black carbon, and sea salt aerosols, providing global distributions of aerosol concentrations, vertical profiles, and optical thickness of individual as well as total aerosols (Chin et al. 2002). Since the coupling of MOZART with GOCART in WRF-Chem, also known as MOZCART, is linked to a model parameter that controls separation between smoldering and flaming emissions within the plume rise model (Freitas et al. 2007; Grell et al. 2011), it is suitable for NWP in continental-scale applications such as large-scale forest fires. Fire regime can affect smoke optical properties and is very important to account for in NWP systems.

Previous studies employing the MOZCART chemistry option in WRF-Chem simulations have demonstrated robust model performance in reproducing dust storms (e.g., Kumar et al. 2014; Nguyen et al. 2019; Zupanski et al. 2019) and wildfire (e.g., Amnuaylojaroen et al. 2014; Mar et al. 2016; Lassman et al. 2017; Singh et al. 2020) events.

The meteorological forecasts are driven by the National Oceanic Atmospheric Administration (NOAA) Global Forecast System (GFS) model data. For the chemistry, National Center for Atmospheric Research (NCAR) Whole Atmosphere Community Climate Model (WACCM; Marsh et al. 2013) forecasts are employed to map the background concentrations of gases and aerosols to the CPTEC WRF-Chem initial and boundary conditions. Both the GFS and WACCM data are provided every 6 h.

For biomass-burning emissions, the modeling system is coupled with the 3BEM (Longo et al. 2010). The 3BEM model is based on near-real-time remote sensing fire products to determine fire emissions and plume rise characteristics of trace gases and aerosol particles from open biomass burning, including wildfires and agricultural fires. The fire database utilized is a combination of the Geostationary Operational Environmental Satellite–Wildfire Automated Biomass Burning Algorithm (GOES WF_ABBA); the Brazilian National Institute for Space Research (INPE) fire product, which is based on the Advanced Very High Resolution Radiometer (AVHRR) on board the NOAA polar-orbiting satellites series; and the MODIS fire product. The locations of the detected fire hotspots are cross tabulated with MODIS-derived land-cover products (e.g., aboveground biomass density), combustion factors, and emission factors from literature (Andreae and Merlet 2001; Houghton et al. 2001; Sestini et al. 2003; Akagi et al. 2011; Pereira et al. 2016). To avoid double counting of the same fire, the three fire products are combined using a filter algorithm (Longo et al. 2010). 3BEM emission fields can be directly interpolated onto WRF-Chem grids by using the PREP-CHEM-SRC (Freitas et al. 2011). The PREP-CHEM-SRC is the CPTEC emissions preprocessor, and is designed to prepare emission fields from a large set of source types and databases to be used in global and regional transport models.

The anthropogenic emissions are based on the Hemisphere Transport of Air Pollution, version 2.2 (HTAPv2.2), emission inventory (Janssens-Maenhout et al. 2015). The HTAPv2.2 is a compilation of different regional gridded inventories and available sources based on nationally reported emission datasets for the 2000–10 period. For South America, HTAPv2.2 emissions are based on the Emissions Database for Global Atmospheric Research, version 4.3 (EDGARv4.3), and are provided as monthly maps on a global basis at a resolution of 10 km. Although anthropogenic sources are commonly regarded as the most important emission sources over urban areas, biogenic emissions can lead (directly or indirectly) to an increase in air pollution levels around and even far from their sources (e.g., Artaxo et al. 2013; Shrivastava et al. 2019). Dust and sea salt emissions are dominant over desert and coastal regions, respectively, but can also modify the atmospheric composition of remote areas when transported long distances away from their sources (e.g., Prospero et al. 2014; Chen et al. 2019). Emissions from nature such as biogenic, dust and sea salt emissions are not considered in the implementation of the CPTEC WRF-Chem; however, these emissions are being evaluated and will be incorporated in the next modeling upgrades.

The CPTEC WRF-Chem modeling system is composed of three principal components (schematic in Fig. 1): preprocessing, forecasting, and postprocessing. The preprocessing defines the modeling domain, interpolates static geographical data to the model grid, and prepares the meteorological, background concentrations, and emission fields to be read during the forecasting. For the experimental setup proposed here, the modeling domain consists of 378 × 402 horizontal grid points at a resolution of 20 km and with 30 vertical layers. The forecasting is a numerical integration program that links, through a reliable dynamic solver, a set of state-of-the-art physical and chemical parameterization schemes with external fields

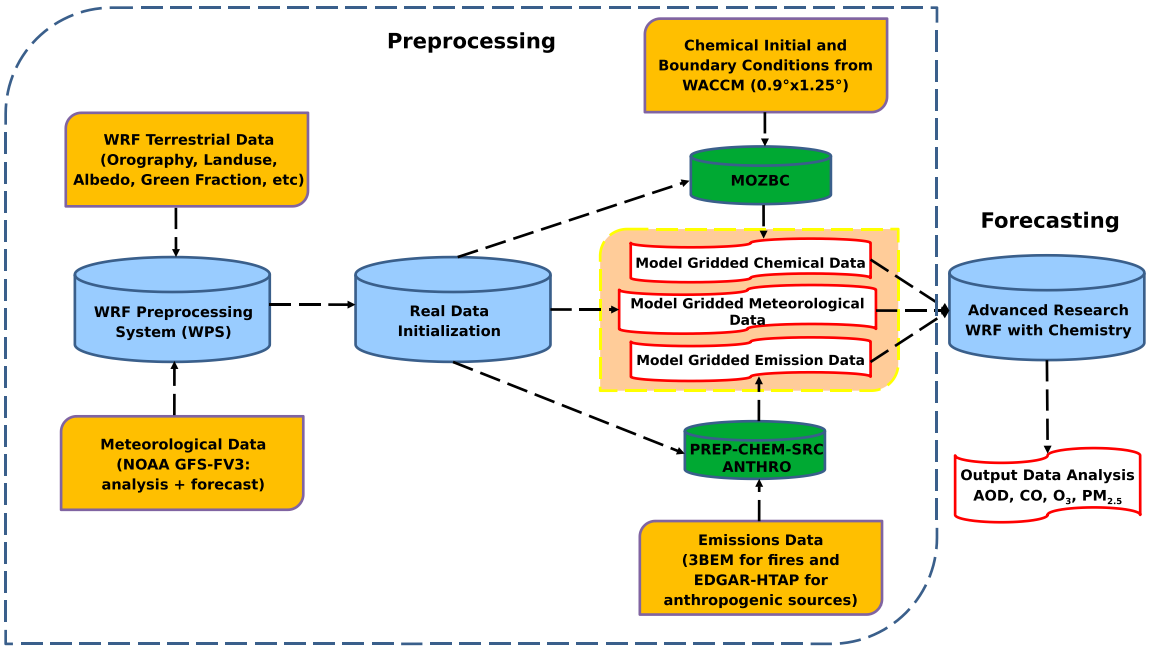

Fig. 1. Schematic representation of the CPTEC WRF-Chem modeling system. The yellow boxes represent the external data, the green boxes the chemical and emissions preprocessing interfaces, and the blue boxes the major components of the system. Air pollution forecasts are carried out with a resolution of 20 km and for a forecast range of 48 h.

prepared during the Preprocessing. The main physics (which are the same as those used in the WRF-ARW-5km for NWP), chemistry, and emission model options and other simulation attributes are listed in Table 1. Once the forecasting section ends, a procedure designed to postprocess the model output and meet specific requirements for storage is applied. A schematic view of the CPTEC WRF-Chem modeling system, including its preprocessing tools, can be seen in Fig. 1.

CPTEC WRF-Chem modeling system performance evaluation

In this paper, we primarily focus on how smoke plumes generated by biomass-burning events observed over the Amazon can spread over substantial portions of the continent and have a considerable effect on both climate and human health. Thus, two experiments of 48-h simulations with an initialization time at 0000 UTC were performed, on a daily basis, during August and September of 2018 and 2019. The experiment in 2019 included the very strong 3-week forest fire event, when the SPMA was plunged into darkness on August 19.

AOD_{550nm} and CO satellite estimates were obtained from the Measurement of Pollution in the Troposphere (MOPITT) and MODIS retrievals, whereas the model data were taken from our in-house WRF-Chem model and the European Centre for Medium-Range Weather Forecasts (ECMWF) Copernicus Atmosphere Monitoring Service (CAMS) model. The MOPITT is a thermal and near-IR nadir-viewing gas filter radiometer with a ground resolution of 22 km × 22 km, and the instrument, measurement, and retrieval techniques are described in detail by Drummond et al. (1992), Edwards et al. (1999), and Deeter et al. (2003), respectively. The MODIS is a 36-channel optical sensor with the ability to characterize the spatial and temporal variability of the global aerosol field and takes images for the entire Earth's surface every 1–2 days with a swath width of 2,330 km. MODIS fundamentals are described in Ackerman et al. (1998) and Gao et al. (2002). MOPITT and MODIS, on board the NASA *Terra* and *Aqua* satellites, respectively, have been operating almost continuously since they were launched in a sun-synchronous orbit, with local equator crossing times of approximately 1030 and 1330 LT. The ECMWF-CAMS AOD_{550nm} and CO total-column data used for

the model comparison have a horizontal resolution of approximately 40 km. Quantitative statistical measures for model evaluation include the mean (M_{obs} and M_{sim}), correlation coefficient (R), standard deviation (σ_{obs} and σ_{sim}), and root-mean-square error (RMSE), as defined in supplement Table ES1. For ease of model–satellite data comparison, the MOPITT, MODIS, and ECMWF-CAMS data were initially regridded to the CPTEC WRF-Chem grid and then averaged in time and space over this grid. Overall, as shown below, the model results were in good agreement with the remote satellite information and surface measurements reported at different São Paulo Environmental Agency (CETESB) monitoring sites in southeastern South America. Several limitations and uncertainties were identified and will help to improve the model's forecast capability in future implementations.

August–September 2018 fire season. We limited our study to the period in which most of the smoke plumes were observed at the peak of the burning season between August and September. Figure 2 shows the temporal mean spatial distributions of AOD_{550nm} and CO total column derived from satellite and model datasets during August and September of 2018 and 2019. The AOD_{550nm} and CO total-column spatial variabilities are reproduced fairly well by the model over the continent. The CPTEC WRF-Chem results are often within ±30% of the MOPITT and MODIS estimates, although significant model overestimations over the western Amazon were observed, with up to 60% of satellite data (see Fig. 2). Model overestimation over the western Amazon can be mainly attributed to uncertainties in the calculation of biomass-burning

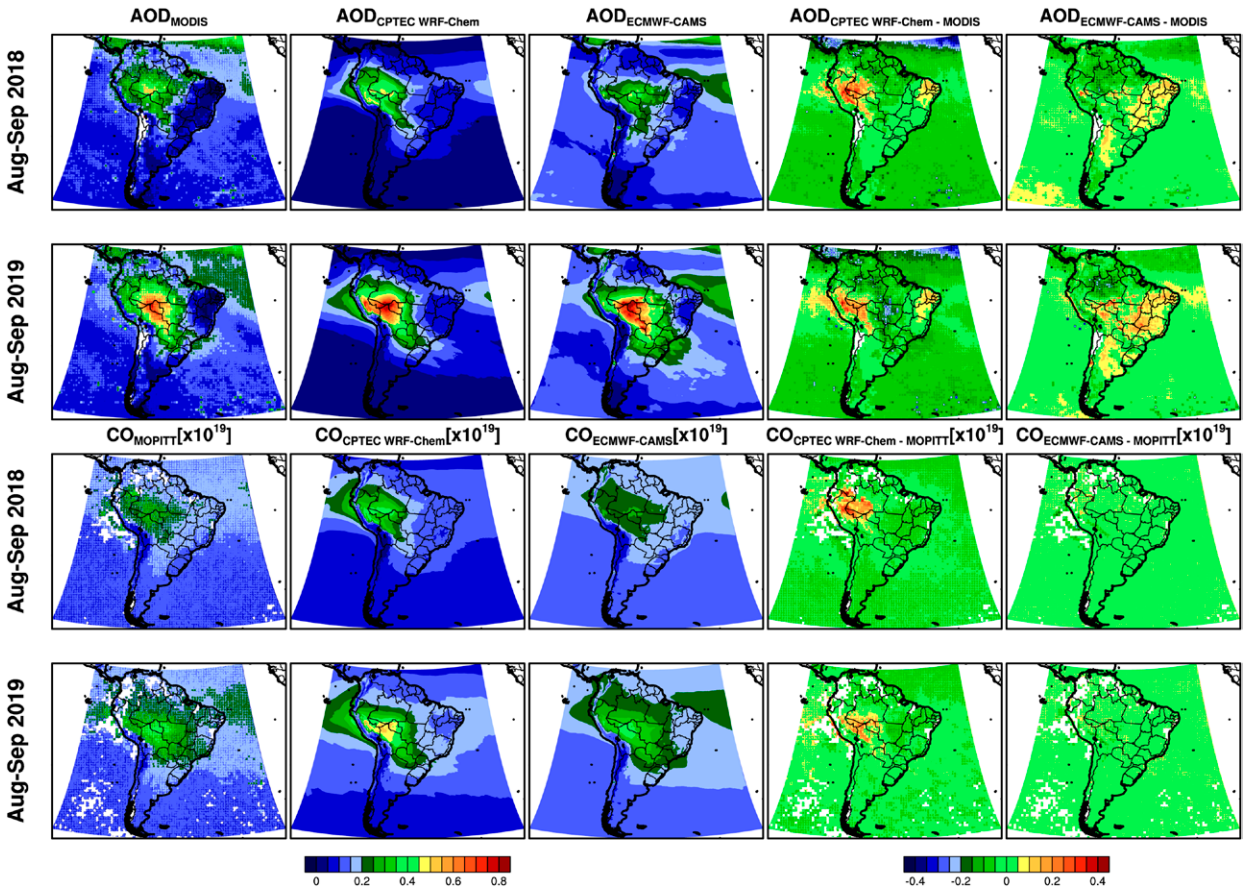

Fig. 2. Temporal mean spatial distributions of AOD_{550nm} and CO total column as retrieved from (column 1) MODIS and MOPITT satellite instruments, and as modeled with the (column 2) CPTEC WRF-Chem and (column 3) ECMWF-CAMS models, averaged over the period from 1 Aug to 30 Sep of 2018 and 2019. Absolute differences between the (column 4) CPTEC WRF Chem and (column 5) ECMWF-CAMS models and satellite datasets. The mean concentrations are calculated on the basis of the MODIS and MOPITT daily retrievals. MOPITT CO units are in mol cm^{-2}.

emissions (e.g., Archer-Nicholls et al. 2015; Pereira et al. 2016) rather than to the representation of meteorological processes. Pereira et al. (2016) pointed out that land-use information over the western Amazon is out-of-date, and that fire emission models that use that information continue to insert fire hotspots even if forest areas had been burned/deforested during earlier years. This result underscores the need for more accurate representations of biomass-burning aerosol emissions to reduce uncertainties in the model predictions. On the other hand, no significant precipitation events were observed and predicted over the western Amazon during August and September 2018 (see Fig. ES3 in the supplement). The CPTEC WRF-Chem AOD_{550nm} underestimations over the ocean are mainly due to two factors: first, online sea salt emission calculations were not included, and second, the inflow of sea salt and dust aerosols from Africa through the boundaries was not taken into account in the simulations. Dust aerosols from the Sahara Desert are more frequently advected to South America during the austral summer; however, significant fractions of smoke transported to South America during the austral winter can also be composed of desert dust aerosols (Mahowald et al. 2014). Table 2 summarizes the CPTEC WRF-Chem performance statistics for the fire season in 2018. The ECMWF-CAMS, a global model with data assimilation system to assimilate observations of atmospheric composition, performed better than the CPTEC WRF-Chem.

Table 2. Performance statistics for 2018.

	CPTEC WRF-Chem		ECMWF-CAMS	
Index	MODIS	MOPITT[a]	MODIS	MOPITT
M_{obs}	0.12	1.42×10^{18}	0.12	1.42×10^{18}
M_{sim}	0.07	1.06×10^{18}	0.13	1.50×10^{18}
R	0.52	0.49	0.57	0.62
σ_{obs}	0.13	5.59×10^{17}	0.13	5.59×10^{17}
σ_{sim}	0.15	9.86×10^{17}	0.11	4.43×10^{17}
RMSE	0.15	9.33×10^{17}	0.11	4.53×10^{17}

[a] MOPITT CO units are in mol cm^{-2}.

August–September 2019 fire season. The 2019 fire season over the Amazon was one of the most intense fire seasons in the last two decades, with the intrusion of smoke plumes coming from Africa (see left panels in Fig. 2), where very intense forest fires events during this period were also observed. As a consequence, more biomass-burning products were injected into the atmosphere over the Amazon and thus transported to southeastern South America (see Fig. ES1 in the supplement). The predicted AOD_{550nm} and CO total-column concentrations over the western Amazon were positively biased relative to the observations, with up to 50% of satellite data (see Fig. 2). Similar to the fire season in 2018, no significant precipitation events were observed and predicted over this region during August and September 2019 (see Fig. ES3 in the supplement), and model–satellite differences can be largely attributed to uncertainties in the calculation of biomass burning emissions. Similar to the fire season in 2018, the CPTEC WRF-Chem AOD_{550nm} underestimations over the northwest Atlantic Ocean are a result of the lack of inclusion of both sea salt and dust aerosols; these aerosol species were not considered online in the simulations or in the description of inflow boundary conditions. The MOPITT CO total-column concentrations were also underestimated by the model over the northwestern Atlantic Ocean, indicating that discrepancies between the model results and the satellite data over that region can be largely attributed to errors in the lateral boundary conditions rather than in the emission calculations. The CPTEC WRF-Chem performance statistics for the fire season in 2019 are summarized in Table 3. The results

Table 3. Performance statistics for 2019.

	CPTEC WRF-Chem		ECMWF-CAMS	
Index	MODIS	MOPITT[a]	MODIS	MOPITT
M_{obs}	0.15	1.64×10^{18}	0.15	1.64×10^{18}
M_{sim}	0.10	1.38×10^{18}	0.17	1.74×10^{18}
R	0.62	0.60	0.67	0.70
σ_{obs}	0.18	7.16×10^{17}	0.17	7.16×10^{17}
σ_{sim}	0.16	8.97×10^{17}	0.17	6.10×10^{17}
RMSE	0.16	7.83×10^{17}	0.14	5.24×10^{17}

[a] MOPITT CO units are in mol cm^{-2}.

obtained with CPTEC WRF-Chem are similar to those from the ECMWF-CAMS. Although some limitations and uncertainties were identified, the CPTEC WRF-Chem modeling system can reproduce the overall aspects of the transport of biomass-burning smoke plumes over South America.

Case study: The SPMA plunged into darkness on 19 August 2019. As mentioned above, fire occurrences exhibit a significant increase in the Amazon during the dry season, with regional smoke plumes that can travel long distances from their sources driven by the South American low-level jet (SALLJ; Marengo et al. 2002), an efficient dynamic mechanism for transporting heat and moisture from the Amazon to the subtropics. The SALLJ has been described by numerous studies as one of the major drivers responsible for transporting biomass-burning products across the Amazon to the subtropical region of South America (Freitas et al. 2009; Ulke et al. 2011; Martins et al. 2018). A typical long-range transport of smoke plumes is clearly shown in Fig. 3 and can be depicted in a very simple way as follows: the smoke plumes that originate in the central Amazon are first transported westward (where the low–midtropospheric circulation is halted by the Andes) and then deflected by the Andes and finally transported southward, reaching midlatitude regions due to the approach of a cold front that confines the smoke plumes to southeastern South America (Ulke et al. 2011).

In the particular event of SALLJ and biomass burning presented in this paper, the incursion of a cold front favored the penetration of the smoke plumes toward southeastern Brazil, arriving at the SPMA on August 19 (see right panels in Fig. 3). Both CPTEC WRF-Chem and ECMWF-CAMS were able to predict the arrival of the smoke plume correctly, with the CPTEC WRF-Chem results being closer to the MODIS estimates (domainwide RMSE and R over the state of São Paulo of 0.23 and 0.56 for CPTEC WRF-Chem against 0.79 and 0.63 for ECMWF-CAMS,

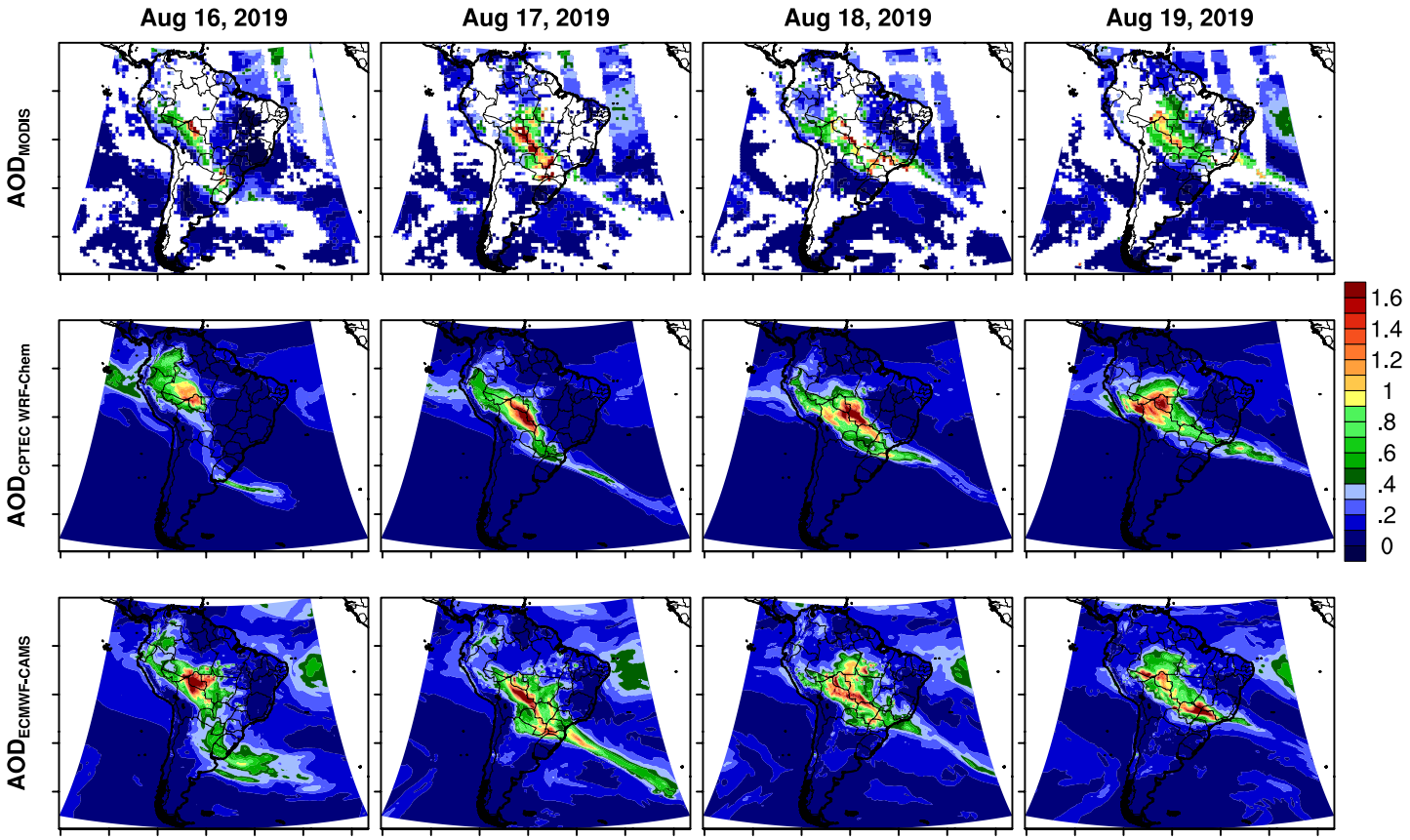

Fig. 3. Spatial distributions of AOD_{550nm} at 1330 LST during the period 16–19 Aug 2019. The AOD_{550nm} estimates are derived from (top) MODIS, (middle) CPTEC WRF-Chem, and (bottom) ECMWF-CAMS datasets.

respectively). Although a very strong smoke transport coming from the Amazon was observed in the middle of the afternoon on 19 August, its impact on atmospheric composition over the SPMA took place in upper levels far above the surface, where, conversely, low air pollutant concentrations were observed (see Fig. 4). Vertical profiles of aerosol extinction derived from model results show that the aerosol layers were mostly confined between 2,000 and 5,000 m in altitude, with the maximum aerosol layering peaking at approximately 1500 LST (see Figs. ES4 and ES5 in the supplement). When aerosol layers are detected above the PBL over the SPMA during the dry season, they may be associated with the long-range transport of particles originating mainly from forest fire events in the Amazon (Lopes et al. 2014; de Miranda et al. 2017; Vara-Vela et al. 2018). Interactions between moist air masses in the warm stage of the cold front with smoke aerosols can enable the formation of tiny cloud droplets, which in turn reflect sunlight back to space, grow larger via water vapor condensation and eventually fall to the ground as rain. According to Fundação de Amparo à Pesquisa do Estado de São Paulo (FAPESP; FAPESP 2019), the sky over the SPMA was suddenly wrapped in a blanket of darkness on August 19, with the sunlight almost completely extinguished by an interaction (that has yet to be fully investigated) between the very intense smoke haze from the north/northwest and the clouds arriving with an Antarctic cold front from the south.

Figure 4 shows the predicted and observed surface concentrations of $PM_{2.5}$, CO, and O_3 at three CETESB monitoring sites during the period from 16 to 19 August 2019. Surface $PM_{2.5}$ and O_3 concentrations were both well reproduced by the model before the arrival of the smoke plume in the afternoon on August 19. In contrast, they were not well represented by the model after this point in time, in part due to the lack of inclusion of wet removal processes (see Fig. ES6 in the supplement). The average R and RMSE were 0.29 and 17.6 μg m^{-3}, respectively, for $PM_{2.5}$ concentrations, and were 0.56 and 29.1 μg m^{-3}, respectively, for O_3 concentrations. Wet scavenging and removal processes due to aqueous-phase chemistry in clouds are not considered in the current version of the system but will be included in its next

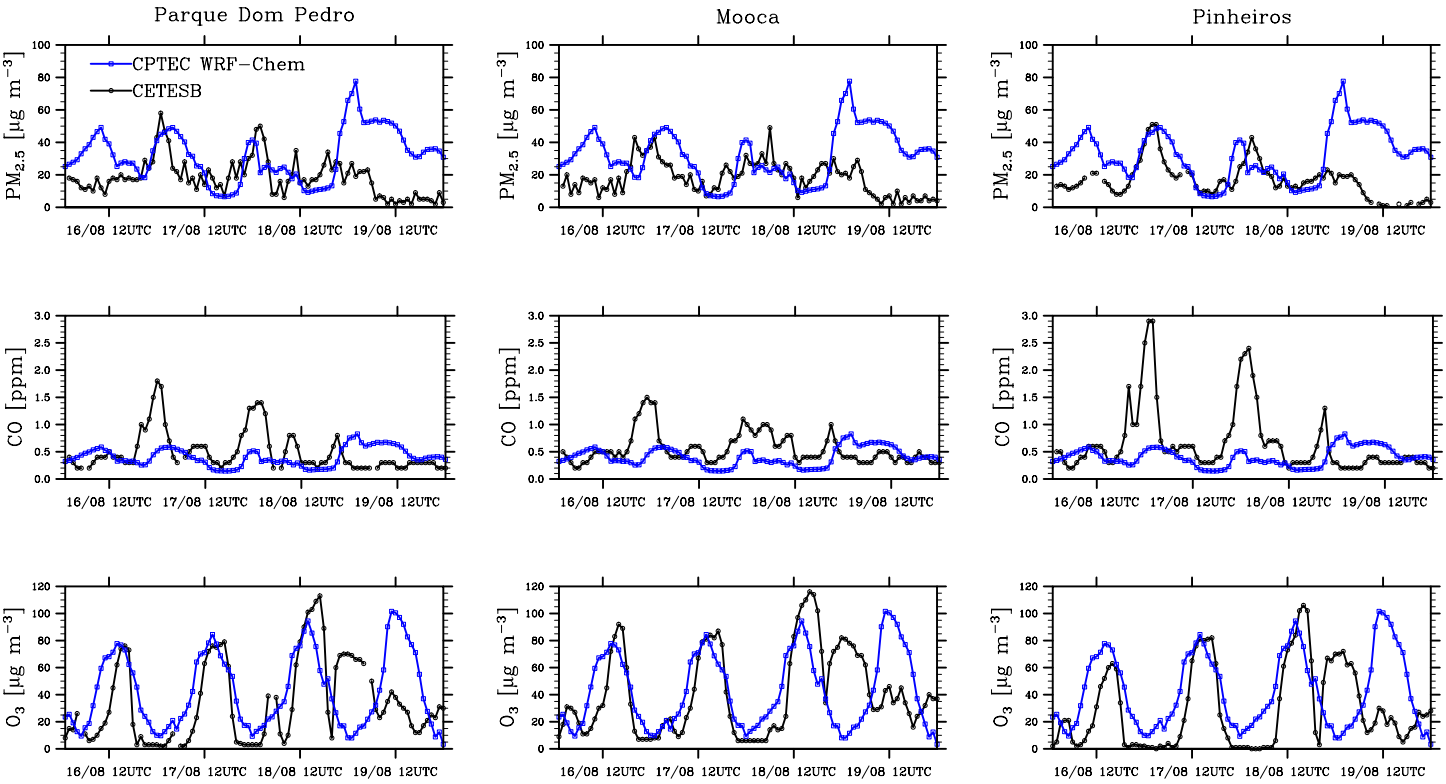

Fig. 4. Predicted (blue dots) and observed (black dots) surface concentrations of $PM_{2.5}$, CO, and O_3 at three São Paulo Environmental Agency (CETESB) monitoring sites during the period from 16 to 19 Aug 2019.

version. In addition to inaccurate predictions of meteorological parameters, the $PM_{2.5}$ model–observation discrepancies are related to uncertainties in the calculation of anthropogenic emissions. Global emission inventories such as EDGAR-HTAP usually have low spatial and temporal resolution and do not represent specific characteristics of urban areas. A detailed description of uncertainties in global emission models can be found in Hoesly et al. (2018). Knowledge gaps in aerosol modeling in terms of formation and aging processes, including aerosol feedbacks on meteorology, represent other sources of uncertainty. Previous studies have suggested that the interactions between meteorological processes and aerosol species can be significant during strong air pollution episodes such as wildfires and dust storms (Chen et al. 2014; Kong et al. 2015; Vara-Vela et al. 2018; Liu et al. 2020). Due to geographical characteristics, no significant contributions of biogenic, dust and sea salt emissions to the $PM_{2.5}$ concentrations over the SPMA are expected. A source apportionment performed by Pereira et al. (2017) shows that road dust, industrial emissions, vehicular exhaust, biomass burning and secondary processes represent the major contributors to the $PM_{2.5}$ concentrations over the SPMA. While biogenic emissions were not considered as input emissions, the chemical evolution of the plumes downwind of fires can be affected by biogenic emissions across smoke plume trajectories (e.g., Hatch et al. 2019). Mismatches between predictions and observations in regard to the timing of peak concentrations depend largely on the inherent constraints in representing the meteorological and emission fields at any particular time and location. For instance, since the EDGAR-HTAP temporal profiles are based on official international statistics, emission characteristics at urban scale for each country cannot always be provided, and instead, a unique temporal profile is often used throughout a country. The underestimation of maximum CO concentrations is largely attributed to uncertainties in the calculation of emissions, mainly those derived from human activities.

Concluding remarks

A new predictive framework for Amazon forest fire smoke dispersion over South America (CPTEC WRF-Chem) has been developed based on the Weather Research and Forecasting with Chemistry community model. Efforts have been focused on the representation of the most important aerosol source over the Amazon during the dry season: biomass burning. Widely recognized as the main contributors to air pollution over urban areas, anthropogenic emission sources were also taken into account as input emissions. The evaluation results indicate that the CPTEC WRF-Chem system for the 48-h forecast during August–September 2018 and 2019 is capable of reproducing the overall spatial and temporal variability of AOD_{550nm} and CO total column, yielding better performance statistics for the fire season with greater biomass-burning activity. The model comparison shows that the ECMWF-CAMS performed better than the CPTEC WRF-Chem, with higher differences between CPTEC WRF-Chem and satellite data being attributed to uncertainties in the fire emissions calculation as well as to missing emission sources (biogenic, dust, and sea salt). Regarding the long-range transport event on August 19, both CPTEC WRF-Chem and ECMWF-CAMS performed fairly well in considering the arrival of the smoke plume at the SPMA, with CPTEC WRF-Chem AOD_{550nm} spatial distribution being closer to MODIS estimates. Overall and in spite of some discrepancies, mainly at site-specific locations, the air quality forecasting system is well suited for the prediction of the spread of fire smoke plumes across South America and is thus able to provide warning alerts several days before the imminence of acute pollution episodes over this region.

In its current configuration (Table 1 and Fig. 1), the system is executed daily immediately after the CPTEC Satellite Division releases the latest available data of active fire locations. The model outputs are postprocessed and then forwarded to a central database. As a final product, the surface and total-column concentrations of key chemical species such as CO, tropospheric ozone and $PM_{2.5}$ are displayed and stored as hourly outputs on the CPTEC website.

Future developments

Some of the interesting prospects that will be investigated and implemented as a continuation of this work are as follows:

- Inclusion of sea salt, dust, and biogenic emission sources; accurate emissions are essential to improving air quality simulations
- Improvements in the 3BEM emission model and tests with the Global Fire Assimilation System (GFAS)
- Tests with the inclusion of aerosol feedbacks on NWP
- Calculation of the air quality index, with a special focus on densely populated areas

In addition, the CPTEC WRF-Chem will be used as a benchmark within the framework of the Chemistry of the Atmosphere–Field Experiment in Brazil (CAFE-Brazil) project. The CAFE-Brazil project is a joint partnership project between Germany and Brazil that will operate in diverse urban environments across the Amazon, focusing on improving our fundamental understanding of the role of aerosol-cloud interactions in the climate system. With the use of a network of observations, including HALO missions, and state-of-the-art modeling tools, CAFE-Brazil partners will work toward reinforcing Brazilian climate and air quality research networks. The CAFE-Brazil project will take place in 2022 over the Amazon.

Acknowledgments. We acknowledge CAPES for partially funding this work through the project CAPES/Modelagem 88881.148662/2017-01. We also acknowledge the National Center for Atmospheric Research for providing the WRF-Chem model, the NASA DAACs for providing the MODIS and MOPITT data, the European Centre for Medium-Range Weather Forecasts for providing the CAMS atmospheric composition data, and the CETESB for providing air quality data. We also thank Wanderson Santos for his support in data processing.

References

Ackerman, S. A., and Coauthors, 1998: Discriminating clear sky from clouds with MODIS. *J. Geophys. Res.*, **103**, 32 141–32 157, https://doi.org/10.1029/1998JD200032.

Akagi, S. K., and Coauthors, 2011: Emission factors for open and domestic biomass burning for use in atmospheric models. *Atmos. Chem. Phys.*, **11**, 4039–4072, https://doi.org/10.5194/acp-11-4039-2011.

Alvim, D. S., and Coauthors, 2017: Aerosol distribution over Brazil with ECHAM-HAM and CAM5-MAM3 simulations and its comparison with ground-based and satellite data. *Atmos. Pollut. Res.*, **8**, 718–728, https://doi.org/10.1016/j.apr.2017.01.008.

Amnuaylojaroen, T., and Coauthors, 2014: Effect of different emission inventories on modeled ozone and carbon monoxide in Southeast Asia. *Atmos. Chem. Phys.*, **14**, 12 983–13 012, https://doi.org/10.5194/acp-14-12983-2014.

Andreae, M. O., and P. Merlet, 2001: Emission of trace gases and aerosols from biomass burning. *Global Biogeochem. Cycles*, **15**, 955–966, https://doi.org/10.1029/2000GB001382.

Aragão, L. E. O. C., and Coauthors, 2008: Interactions between rainfall, deforestation and fires during recent years in the Brazilian Amazonia. *Philos. Trans. Roy. Soc.*, **363**, 1779–1785, https://doi.org/10.1098/rstb.2007.0026.

Archer-Nicholls, A., and Coauthors, 2015: Characterising Brazilian biomass burning emissions using WRF-Chem with MOSAIC sectional aerosol. *Geosci. Model Dev.*, **8**, 549–577, https://doi.org/10.5194/gmd-8-549-2015.

Artaxo, P., and Coauthors, 2002: Physical and chemical properties of aerosols in the wet and dry seasons in Rondônia, Amazonia. *J. Geophys. Res.*, **287**, 8081, https://doi.org/10.1029/2001JD000666.

——, and Coauthors, 2013: Atmospheric aerosols in Amazonia and land use change: From natural biogenic to biomass burning conditions. *Faraday Discuss.*, **165**, 203–235, https://doi.org/10.1039/c3fd00052d.

Barlow, J., E. Berenguer, R. Carmenta, and F. França, 2019: Clarifying Amazonia's burning crisis. *Global Change Biol.*, **26**, 319–321, https://doi.org/10.1111/gcb.14872.

Belcher, C. M., 2013: *Fire Phenomena and the Earth System: An Interdisciplinary Guide to Fire Science*. Wiley, 352 pp.

Cardil, A., and Coauthors, 2020: Recent deforestation drove the spike in Amazonian fires. *Environ. Res. Lett.*, **15**, 121003, https://doi.org/10.1088/1748-9326/abcac7.

Chen, S., and Coauthors, 2014: Regional modeling of dust mass balance and radiative forcing over East Asia using WRF-Chem. *Aeolian Res.*, **15**, 15–30, https://doi.org/10.1016/j.aeolia.2014.02.001.

Chen, Y., and Coauthors, 2019: Natural sea-salt emissions moderate the climate forcing of anthropogenic nitrate. *Atmos. Chem. Phys.*, **20**, 771–786, https://doi.org/10.5194/acp-2019-556.

Chin, M., R. B. Rood, S.-J. Lin, J.-F. Müller, and A. M. Thompson, 2000: Atmospheric sulfur cycle simulated in the global model GOCART: Model description and global properties. *J. Geophys. Res.*, **105**, 24 671–24 687, https://doi.org/10.1029/2000JD900384.

——, and Coauthors, 2002: Tropospheric aerosol optical thickness from the GOCART model and comparisons with satellite and sun photometer measurements. *J. Atmos. Sci.*, **59**, 461–483, https://doi.org/10.1175/1520-0469(2002)059<0461:TAOTFT>2.0.CO;2.

Deeter, M. N., and Coauthors, 2003: Operational carbon monoxide retrieval algorithm and selected results for the MOPITT instrument. *J. Geophys. Res.*, **108**, 4399, https://doi.org/10.1029/2002JD003186.

de Magalhães, N., H. Evangelista, T. Condom, A. Rabatel, and P. Ginot, 2019: Amazonian biomass burning enhances tropical Andean glaciers melting. *Sci. Rep.*, **9**, 16914, https://doi.org/10.1038/s41598-019-53284-1.

de Miranda, R. M., F. Lopes, N. É. do Rosário, M. A. Yamasoe, E. Landulfo, and M. de Fatima Andrade, 2017: The relationship between aerosol particles chemical composition and optical properties to identify the biomass burning contribution to fine particles concentration: A case study for São Paulo city, Brazil. *Environ. Monit. Assess.*, **189**, 6, https://doi.org/10.1007/s10661-016-5659-7.

Devecchi, M. F., and Coauthors, 2020: Beyond forests in the Amazon: Biogeography and floristic relationships of the Amazonian savannas. *Bot. J. Linn. Soc.*, **20**, 478–503, https://doi.org/10.1093/botlinnean/boaa025.

Drummond, J. R., and Coauthors, 1992: Measurements of Pollution in the Troposphere (MOPITT). *The Use of EOS for Studies of Atmospheric Physics*, J. C. Gille and G. Visconti, Eds., North-Holland, 77–101.

Edwards, D. P., and Coauthors, 1999: Radiative transfer modeling for the EOS Terra satellite Measurement of Pollution in the Troposphere (MOPITT) instrument. *J. Geophys. Res.*, **104**, 16 755–16 775, https://doi.org/10.1029/1999JD900167.

Emmons, L. K., and Coauthors, 2010: Description and evaluation of the Model for Ozone and Related Chemical Tracers, version 4 (MOZART-4). *Geosci. Model Dev.*, **3**, 43–67, https://doi.org/10.5194/gmd-3-43-2010.

Eric, J., and Coauthors, 2018: Realtime wildfire smoke prediction in the United States: The HRRR-Smoke model. EGU General Assembly, Vienna, Austria, Abstract EGU2018-19526.

FAPESP, 2019: Fundação de Amparo à Pesquisa do Estado de São Paulo. Accessed August 2019, http://agencia.fapesp.br/researchers-help-tracing-river-of-smoke-that-blackened-the-day-in-sao-paulo/31290/.

Freitas, S. R., and Coauthors, 2005: Monitoring the transport of biomass burning emissions in South America. *Environ. Fluid Mech.*, **5**, 135–167, https://doi.org/10.1007/s10652-005-0243-7.

——, and Coauthors, 2007: Including the sub-grid scale plume rise of vegetation fires in low resolution atmospheric transport models. *Atmos. Chem. Phys.*, **7**, 3385–3398, https://doi.org/10.5194/acp-7-3385-2007.

——, and Coauthors, 2009: The Coupled Aerosol and Tracer Transport Model to the Brazilian Developments on the Regional Atmospheric Modeling System (CATT-BRAMS)—Part 1: Model description and evaluation. *Atmos. Chem. Phys.*, **9**, 2843–2861, https://doi.org/10.5194/acp-9-2843-2009.

——, and Coauthors, 2011: PREP-CHEM-SRC—1.0: A preprocessor of trace gas and aerosol emission fields for regional and global atmospheric chemistry models. *Geosci. Model Dev.*, **4**, 419–433, https://doi.org/10.5194/gmd-4-419-2011.

Gao, B.-C., and Coauthors, 2002: Distinguishing tropospheric aerosols from thin cirrus clouds for improved aerosol retrievals using the ratio of 1.38-μm and 1.24-μm channels. *Geophys. Res. Lett.*, **29**, 1890, https://doi.org/10.1029/2002GL015475.

Gonzalez-Alonso, L., M. val Martin, and R. A. Kahn, 2019: Biomass-burning smoke heights over the Amazon observed from space. *Atmos. Chem. Phys.*, **19**, 1685–1702, https://doi.org/10.5194/acp-19-1685-2019.

Grell, G. A., S. E. Peckham, R. Schmitz, S. A. McKeen, G. Frost, W. C. Skamarock, and B. Eder, 2005: Fully coupled "online" chemistry within the WRF Model. *Atmos. Environ.*, **39**, 6957–6975, https://doi.org/10.1016/j.atmosenv.2005.04.027.

——, S. R. Freitas, M. Stuefer, and J. Fast, 2011: Inclusion of biomass burning in WRF-Chem: Impact of wildfires on weather forecasts. *Atmos. Chem. Phys.*, **11**, 5289–5303, https://doi.org/10.5194/acp-11-5289-2011.

Hatch, L. E., and Coauthors, 2019: Highly speciated measurements of terpenoids emitted from laboratory and mixed-conifer forest prescribed fires. *Environ. Sci. Technol.*, **53**, 9418–9428, https://doi.org/10.1021/acs.est.9b02612.

Hoelzemann, J. J., K. M. Longo, R. M. Fonseca, N. M. E. do Rosário, H. Elbern, S. R. Freitas, and C. Pires, 2009: Regional representativity of AERONET observation sites during the biomass burning season in South America determined by correlation studies with MODIS aerosol optical depth. *J. Geophys. Res.*, **114**, D13301, https://doi.org/10.1029/2008JD010369.

Hoesly, R. M., and Coauthors, 2018: Historical (1750–2014) anthropogenic emissions of reactive gases and aerosols from the Community Emissions Data System (CEDS). *Geosci. Model Dev.*, **11**, 369–408, https://doi.org/10.5194/gmd-11-369-2018.

Houghton, R. A., and Coauthors, 2001: The spatial distribution of forest biomass in the Brazilian Amazon: A comparison of estimates. *Global Change Biol.*, **7**, 731–746, https://doi.org/10.1046/j.1365-2486.2001.00426.x.

Ichoku, C., R. Kahn, and M. Chin, 2012: Satellite contributions to the quantitative characterization of biomass burning for climate modeling. *Atmos. Res.*, **111**, 1–28, https://doi.org/10.1016/j.atmosres.2012.03.007.

Janssens-Maenhout, G., and Coauthors, 2015: HTAP_v2.2: A mosaic of regional and global emission grid maps for 2008 and 2010 to study hemispheric transport of air pollution. *Atmos. Chem. Phys.*, **15**, 11 411–11 432, https://doi.org/10.5194/acp-15-11411-2015.

Kganyago, M., and Coauthors, 2020: Assessment of the characteristics of recent major wildfires in the USA, Australia and Brazil in 2018–2019 using multi-source satellite products. *Remote Sens.*, **12**, 1803, https://doi.org/10.3390/rs12111803.

Kong, X., and Coauthors, 2015: Analysis of meteorology–chemistry interactions during air pollution episodes using online coupled models within AQMEII phase-2. *Atmos. Environ.*, **115**, 527–540, https://doi.org/10.1016/j.atmosenv.2014.09.020.

Kumar, R., and Coauthors, 2014: WRF-Chem simulations of a typical pre-monsoon dust storm in northern India: Influences on aerosol optical properties and radiation budget. *Atmos. Chem. Phys.*, **14**, 2431–2446, https://doi.org/10.5194/acp-14-2431-2014.

Lassman, W., and Coauthors, 2017: Spatial and temporal estimates of population exposure to wildfires smoke during the Washington State 2012 wildfire season using blended model, satellite, and in situ data. *Geohealth*, **1**, 106–121, https://doi.org/10.1002/2017GH000049.

Liu, L., and Coauthors, 2020: Impact of biomass burning aerosols on radiation, clouds, and precipitation over the Amazon: Relative importance of aerosol–cloud and aerosol–radiation interactions. *Atmos. Chem. Phys.*, **20**, 13 283–13 301, https://doi.org/10.5194/acp-20-13283-2020.

Lizundia-Loiola, J., and Coauthors, 2020: Temporal anomalies in burned area trends: Satellite estimations of the Amazonian 2019 fire crisis. *Remote Sens.*, **12**, 151, https://doi.org/10.3390/rs12010151.

Longo, K. M., S. R. Freitas, M. O. Andreae, A. Setzer, E. Prins, and P. Artaxo, 2010: The Coupled Aerosol and Tracer Transport Model to the Brazilian Developments on the Regional Atmospheric Modeling System (CATT-BRAMS)—Part 2: Model sensitivity to the biomass burning inventories. *Atmos. Chem. Phys.*, **10**, 5785–5795, https://doi.org/10.5194/acp-10-5785-2010.

Lopes, F., G. Moreira, P. Rodrigues, J. L. Guerrero-Rascado, M. Andrade, and E. Landulfo, 2014: Lidar measurements of tropospheric aerosol and water vapor profiles during the winter season campaigns over the metropolitan area of São Paulo, Brazil. *Proc. SPIE*, **9246**, 92460H, https://doi.org/10.1117/12.2067374.

Mahowald, N., S. Albani, J. F. Kok, S. Engelstaeder, R. Scanza, D. S. Ward, and M. G. Flanner, 2014: The size distribution of desert dust aerosols and its impact on the Earth system. *Aeolian Res.*, **15**, 53–71, https://doi.org/10.1016/j.aeolia.2013.09.002.

Mar, K. A., and Coauthors, 2016: Ozone air quality simulations with WRF-Chem (v3.5.1) over Europe: Model evaluation and chemical mechanism comparison. *Geosci. Model Dev.*, **9**, 3699–3728, https://doi.org/10.5194/gmd-9-3699-2016.

Marengo, J. A., M. W. Douglas, and P. L. Silva Dias, 2002: The South American low-level jet east of the Andes during the 1999 LBA-TRMM and LBA-WET AMC campaign. *J. Geophys. Res.*, **107**, 8079, https://doi.org/10.1029/2001JD001188.

Marsh, D. R., M. J. Mills, D. E. Kinnison, J.-F. Lamarque, N. Calvo, and L. M. Polvani, 2013: Climate change from 1850 to 2005 simulated in CESM1(WACCM). *J. Climate*, **26**, 7372–7391, https://doi.org/10.1175/JCLI-D-12-00558.1.

Martins, L. D., and Coauthors, 2018: Long-range transport of aerosols from biomass burning over southeastern South America and their implications on air quality. *Aerosol Air Qual. Res.*, **18**, 1734–1745, https://doi.org/10.4209/aaqr.2017.11.0545.

Morgan, W. T., and Coauthors, 2019: Non-deforestation drivers of fires are increasingly important sources of aerosol and carbon dioxide emissions across Amazonia. *Sci. Rep.*, **9**, 16975, https://doi.org/10.1038/s41598-019-53112-6.

Nguyen, H. D., and Coauthors, 2019: Dust storm event of February 2019 in central and east coast of Australia and evidence of long-range transport to New Zealand and Antarctica. *Atmosphere*, **10**, 653, https://doi.org/10.3390/atmos10110653.

Pacifico, F., G. A. Folberth, S. Sitch, J. M. Haywood, L. V. Rizzo, F. F. Malavelle, and P. Artaxo, 2015: Biomass burning related ozone damage on vegetation over the Amazon forest: A model sensitivity study. *Atmos. Chem. Phys.*, **15**, 2791–2804, https://doi.org/10.5194/acp-15-2791-2015.

Pereira, G., and Coauthors, 2016: Assessment of fire emission inventories during the South American Biomass Burning Analysis (SAMBBA) experiment. *Atmos. Chem. Phys.*, **16**, 6961–6975, https://doi.org/10.5194/acp-16-6961-2016.

——, and Coauthors, 2017: Particulate pollutants in the Brazilian city of São Paulo: 1-year investigation for the chemical composition and source apportionment. *Atmos. Chem. Phys.*, **17**, 11 943–11 969, https://doi.org/10.5194/acp-17-11943-2017.

Petersen, A. K., and Coauthors, 2019: Ensemble forecasts of air quality in eastern China—Part 2: Evaluation of the MarcoPolo–Panda prediction system, version 1. *Geosci. Model Dev.*, **12**, 1241–1266, https://doi.org/10.5194/gmd-12-1241-2019.

Prospero, J. M., and Coauthors, 2014: Characterizing the annual cycle of African dust transport to the Caribbean Basin and South America and its impact on the environment and air quality. *Global Biogeochem. Cycles*, **28**, 757–773, https://doi.org/10.1002/2013GB004802.

Reddington, C. L., E. W. Butt, D. A. Ridley, P. Artaxo, W. T. Morgan, H. Coe, and D. V. Spracklen, 2015: Air quality and human health improvements from reductions in deforestation-related fire in Brazil. *Nat. Geosci.*, **8**, 768–771, https://doi.org/10.1038/ngeo2535.

Sestini, M., and Coauthors, 2003: Mapa de cobertura da terra da Amazônia legal para uso em modelos atmosféricos. *Simpósio Brasileiro de Sensoriamento Remoto*, Belo Horizonte, Brazil, SBSR, 2901–2906.

Shrivastava, M., and Coauthors, 2019: Urban pollution greatly enhances formation of natural aerosols over the Amazon rainforest. *Nat. Commun.*, **10**, 1046–1058, https://doi.org/10.1038/s41467-019-08909-4.

Singh, P., P. Sarawade, and B. Adhikary, 2020: Carbonaceous aerosol from open burning and its impact on regional weather in South Asia. *Aerosol Air Qual. Res.*, **20**, 419–431, https://doi.org/10.4209/aaqr.2019.03.0146.

Skamarock, W. C., and Coauthors, 2008: A description of the Advanced Research WRF version 3. NCAR Tech. Note NCAR/TN-475+STR, 113 pp., https://doi.org/10.5065/D68S4MVH.

Solazzo, E., and Coauthors, 2017: Evaluation and error apportionment of an ensemble of atmospheric chemistry transport modeling systems: Multivariable temporal and spatial breakdown. *Atmos. Chem. Phys.*, **17**, 3001–3054, https://doi.org/10.5194/acp-17-3001-2017.

Tyukavina, A., and Coauthors, 2017: Types and rates of forest disturbances in Brazilian Legal Amazon, 2000–2013. *Sci. Adv.*, **3**, e1601047, https://doi.org/10.1126/sciadv.1601047.

Ulke, A. G., K. M. Longo, and S. R. Freitas, 2011: Biomass burning in South America: Transport patterns and impacts. *Biomass—Detection, Production and Usage*, D. Matovic, Ed., InTech, 337–408.

Vara-Vela, A., M. de Fátima Andrade, Y. Zhang, P. Kumar, R. Y. Ynoue, C. E. Souto-Oliveira, F. J. da Silva Lopes, and E. Landulfo, 2018: Modeling of atmospheric aerosol properties in the São Paulo metropolitan area: Impact of biomass burning. *J. Geophys. Res. Atmos.*, **123**, 9935–9956, https://doi.org/10.1029/2018JD028768.

Voiland, A., 2019: Uptick in Amazon fire activity in 2019. NASA, accessed August 2019, https://earthobservatory.nasa.gov/images/145498/uptick-in-amazon-fire-activity-in-2019.

Zupanski, M., and Coauthors, 2019: Impact of atmospheric and aerosol optical depth observations on aerosol initial conditions in a strongly-coupled data assimilation system. *Atmos. Chem. Phys. Discuss.*, https://doi.org/10.5194/acp-2019-2.